



TITLE:

# Reversion Characteristics in an Al-4wt%Cu Alloy

AUTHOR(S):

OSAMURA, Kozo; FURUICHI, Shigeki; KANBAYASHI, Kan; TAKAMUKU, Seizo; MURAKAMI, Yotaro

---

CITATION:

OSAMURA, Kozo ...[et al]. Reversion Characteristics in an Al-4wt%Cu Alloy. *Memoirs of the Faculty of Engineering, Kyoto University* 1978, 40(3): 115-135

ISSUE DATE:

1978-07

URL:

<http://hdl.handle.net/2433/281071>

RIGHT:

# Reversion Characteristics in an Al-4wt%Cu Alloy

By

Kozo OSAMURA†, Shigeki FURUICHI\*, Kan KANBAYASHI\*\*,  
Seizo TAKAMUKU\*\*\* and Yotaro MURAKAMI†

(Received March 16, 1978)

## Abstract

The X-ray diffuse scattering intensity around the 110 reciprocal lattice point was measured in order to determine quantitatively the amount and size of precipitates during ageing and reversion. The precipitated phase was definitely determined by the aids of Laue X-ray photographs and the electron diffraction patterns. The electrical resistivity was carefully measured. When the alloy was aged for 1000 min at 373K, the GP zones precipitated with a mean diameter of 8.0 nm. During the reversion, those zones dissolved perfectly above 458K, which is in good agreement with the result of Beton and Rollason. After the perfect dissolution of the GP zones, the  $\theta'$  phase precipitated directly and heterogeneously. By ageing for 4000 min at 408K, the  $\theta''$  phase precipitated with a mean diameter of 12.5 nm. When its aged alloy was reverted, the temperature at which the volume fraction of precipitates becomes minimum, but not zero, was 498K, where the successively precipitated  $\theta'$  phase existed already.

## I. Introduction

Since GP zones were detected in the age-hardening Al-Cu alloy independently by Guinier<sup>1)</sup> and Preston<sup>2)</sup> in 1938, many studies have been concentrated on the structure and thermal stability as well as on the kinetics of ageing process<sup>3)</sup>. In the present alloy, some kinds of intermediate phases, namely GP zones,  $\theta''$  and  $\theta'$  phases have been recognized to precipitate. The study of reversion was first done by Gayler<sup>4)</sup> in 1922. Later the reversion phenomena were made clear to be the redissolution process of GP zones and/or intermediate phases through heating at

† Department of Metallurgy

\* Department of Metallurgy

Present address: Nippon Kokan K. K., Kawasaki

\*\* Department of Metallurgy,

Present address: Furukawa Aluminium Co., Nikko

\*\*\* Department of Metallurgy,

Present address: Sumitomo Electric Co., Itami

higher temperature<sup>5)</sup>.

Meijering<sup>6)</sup> and Baur<sup>7)</sup> examined theoretically the thermal stability of GP zones on the basis of thermodynamics. Baur suggested that the solvus curve of the zones depends on the size and the reversion temperature, that is, the upper limit of temperature for the existence of zones is 478K for the zones with an infinite diameter in the Al-4wt%Cu alloy. Beton and Rollason<sup>8)</sup> determined the intermediate phase diagram of the GP zones and the  $\theta''$  phase from the measurement of hardness. In the Al-4wt%Cu alloy, the reversion temperature of zones after ageing for 10 days at room temperature is 455K, and its temperature for  $\theta''$  precipitates after ageing for 10 days at 408K is 511K. Prakash and Nijhawan<sup>9)</sup> reported that the hardness of the Al-4wt%Cu alloy naturally aged for about  $4 \times 10^4$  hours recovered completely at 473K, but only partly at 443K.

On the other hand, the result of thermal analysis reported by Iwasaki and Hirano<sup>10)</sup> showed that the stability of GP zones depended on the preceding heat treatment, namely on the ageing condition. The zones precipitated at 543K were not reverted until 633K in the Al-4wt%Cu alloy. Also the study on mechanical properties by Asano and Hirano<sup>11)</sup> indicated that higher ageing temperatures resulted in higher reversion temperatures of the GP zones. The highest reversion temperature in the Al-4wt%Cu alloy after ageing at 403K was 548K. Hori and Hirano<sup>12)</sup> reported that the reversion temperature of the GP zones was 673K in the Al-4wt%Cu alloy. As mentioned above, the reversion temperatures of GP zones proposed by various investigators have wide variations. The reasons for such discrepancies are understood as follows. As pointed out by Graf<sup>13)</sup>, it should be exactly determined whether the change comes from a complete reversion or from a partial reversion depending on the successive precipitation of a more stable phase<sup>8)</sup>, as well as the identification of the reverting metastable phase<sup>12)</sup>. Also, an other cause seems to arise from inaccuracy about the confirmation of precipitated phases during the preceding ageing treatment. As shown in Fig. 1, at room temperature, only the GP zones precipitate, but never the other intermediate phases present, until after ageing a very long time<sup>14)</sup>. At 403K, however, the GP zones precipitate during the initial stage of ageing, and after ageing about 1000 min, the  $\theta''$  phase appears and the GP zones will disappear<sup>15), 16), 17)</sup>. Accordingly, the reversion test after a transitional ageing will give us results about the reversion behavior of two different kinds of intermediate phases<sup>11)</sup>.

Shimizu and Kimura<sup>18)</sup> studied the kinetics of reversion by analysing the change of electrical resistivity during reversion. They found out that the activation energy at the first stage of reversion is smaller than the activation energy for the diffusion of the Cu solute atom in the Al matrix. This means that the diffusion of the Cu

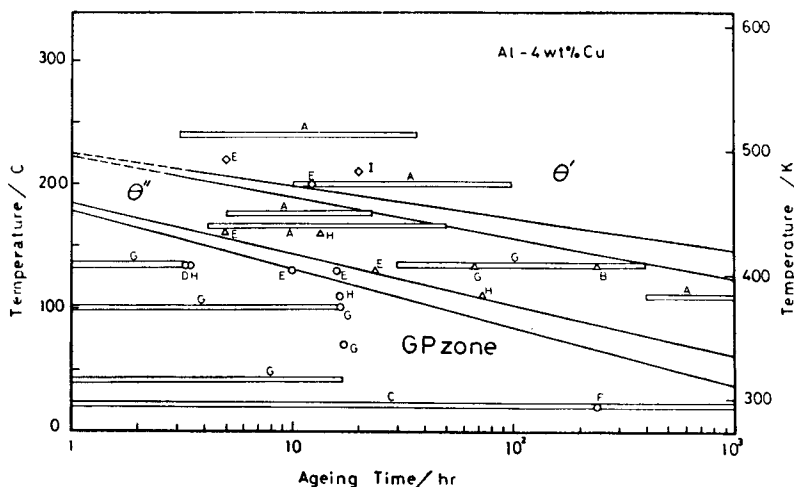


Fig. 1 Summary on the single phase region for GP zone,  $\theta''$  or  $\theta'$  metastable phase in the Al-4wt%Cu alloy aged after the homogenization treatment between 793 and 823K and the quenching into water, where the signs A to I show the following references; A: Boyd and Nicholson (1971)<sup>27</sup>, B: Beton and Rollason (1957-58)<sup>8</sup>, C: Hardy and Heal (1955)<sup>14</sup>, D: Hirouchi et al (1973)<sup>25</sup>, E: Nicholson and Nutting (1958)<sup>41</sup>, F: Silcock et al (1953)<sup>15</sup>, G: Present Work, H: Nakamura et al (1977)<sup>43</sup>, I: Hosford and Agrawal (1975)<sup>44</sup>.

solute atom takes place with the aid of excess vacancies even in the reversion process. Up to the present time, several mechanisms by which the excess vacancies are continuously emitted in the matrix have been suggested<sup>31</sup>. During reversion, excess vacancies are shown to exist in the matrix<sup>20,21</sup>, which are in equilibrium with the line tension of dislocation loops (vacancy cluster mechanism). Another mechanism<sup>22,23</sup> explains that the excess vacancy trapped by the GP zones is slowly released during reversion. Shimizu and Kimura mentioned that the latter vacancy trap mechanism is not effective in the first stage of reversion. However, little study has been done on the kinetics in the later stage of reversion.

In the present work, the X-ray diffuse scattering measurement was performed in order to measure quantitatively the amount and size of precipitates during ageing and reversion. The identification of the precipitated phase was carried out by examining the X-ray Laue photograph and the pattern of electron diffraction. At the same time, the absolute value of electrical resistivity was measured. The reversion behavior in the Al-Cu alloy has been discussed.

## II. Experimental Method

An Al-4.0wt%Cu alloy had been prepared from the starting materials of 99.99%Al and 99.999%Cu. A single crystal for X-ray measurement was prepared by the strain

annealing method, and cut out in dimensions of  $10 \times 20 \times 0.6$  mm<sup>3</sup> with a surface normal of  $\langle 100 \rangle$ . Its plate was chemically etched with a solution of NaOH. The final thickness of the specimen was about 0.45 mm. The wire specimen with a diameter of 1 mm and a length of 150 mm for electrical resistivity measurement was made by drawing a part of the same ingot. Thin foils for the transmission electron microscope (TEM) observation was obtained by electropolishing. The electrolyte was a mixture of 30% nitric acid and 70% methanol, and cooled under 243K.

The specimen was quenched and held in ice-water for 5 seconds after homogenization treatment at 823K for 2 hours, and then placed in liquid nitrogen. The ageing and reversion treatments were performed in a silicon oil bath. The electrical resistivity was measured by the ordinary DC method at liquid nitrogen temperature. All the X-ray measurements were done at room temperature.

The precipitated phase during ageing or reversion was identified from the distinctive patterns of diffuse scattering which appeared in Laue photographs<sup>15)</sup> and the electron diffraction pattern. The diffuse scattering intensity around 110 reciprocal lattice point was measured in order to determine the quantity of precipitates and their mean size. The characteristic X-ray (40kV 20mA) was MoK $\alpha$  reflected from the quartz monochromator. The present method for measuring the diffuse scattering was similar to that reported by Baur and Gerold<sup>24)</sup>, and the details of construction were mentioned in the reference<sup>25)</sup>. In the present measurement, the trace of the Ewald sphere moves on the straight line from point 220 toward the origin. Accordingly, by using the line collimation, the intensity can be observed on the straight line around 110 after the precise determination of position at the 220 point.

### III. Experimental Results

#### III-1. X-Ray Measurement

##### (1) Ageing Process

The diffuse scattering intensity around the 110 reciprocal point for the aged alloy at 408K is shown in Fig. 2. During the early stage of ageing, the intensity profile was rather broad and symmetric. From the Laue photo and TEM observation, the GP zones were confirmed to precipitate only up to 500 min. Beyond 1000 min, the  $\theta''$  phase appeared and its quantity increased remarkably. At 4000 min, all precipitates were of the  $\theta''$  phase. Over 20000 min ageing, the intensity profile became sharp, because of the precipitation of the  $\theta'$  phase. At 70000 min, the quantity of the  $\theta'$  precipitates was greater than that of the  $\theta''$  precipitates.

The total amount of copper atoms included in precipitates is proportional to the integrated intensity, which is the area of the intensity profile<sup>24)</sup>. The present scattering intensity is related to GP zones and  $\theta''$  precipitates, and is also a part of

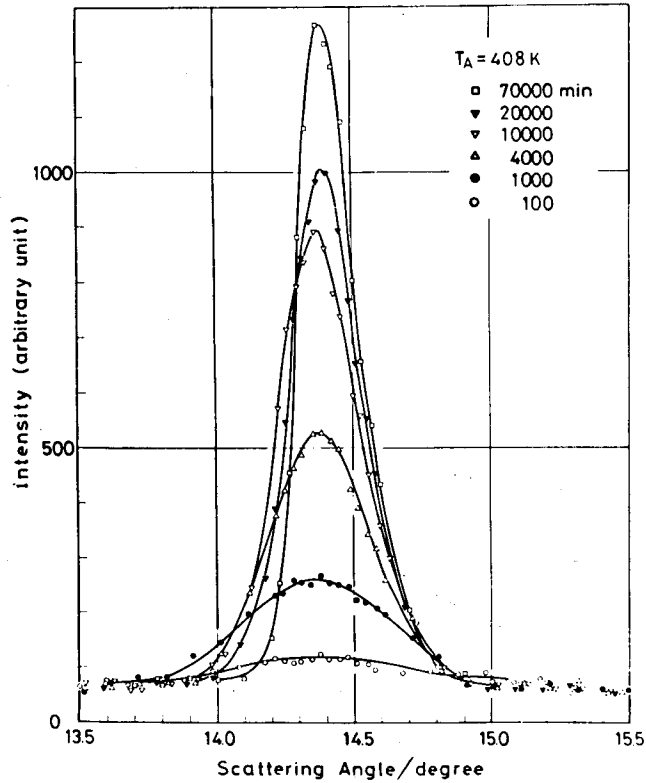


Fig. 2 Diffuse scattering around the 110 reciprocal point in the alloy aged at 408K.

the Bragg scattering by the  $\theta'$  phase<sup>15)</sup>. When those three kinds of particles are assumed to have a disc-like form and a same diameter, the relative contribution to the diffuse scattering intensity around the 110 reciprocal point from one copper atom included in the GP zone, the  $\theta''$  and  $\theta'$  precipitates were estimated to be 1, 2 and 0.02 $N_z$ , respectively. The configuration of copper atoms toward the thickness was assumed as follows. The GP zone has a monolayer sheet of Cu atoms<sup>26)</sup> and the  $\theta''$  phase includes two Cu layers per one precipitate<sup>17), 26)</sup>. The  $\theta'$  precipitate has  $N_z$  unit cells. As the axial ratio for the  $\theta'$  precipitate is 45<sup>27)</sup> and the diameter is about 50 to 100 nm,  $N_z$  was estimated to be 10 to 20. Therefore, the contribution to the diffuse scattering intensity from the  $\theta'$  precipitate is smaller in comparison with other precipitates.

The mean diameter of precipitates is obtained from the Guinier plot on the scattering intensity<sup>24)</sup>. The dimension of the unit cell was taken constantly as 0.404 nm for all three kinds of particles<sup>15)</sup>, although the  $\theta'$  precipitate has a f. c. t. structure with  $a=0.404$  and  $b=0.58$  nm. After ageing for a long time, for example,

at 50000 min ageing, the TEM observation clarified that both the  $\theta'$  and  $\theta''$  precipitates coexisted, and that the diameter of the major  $\theta''$  precipitates reached 20.0 nm. It should be noted that the determination of such a large size is very difficult by the present Guinier plot.

Fig. 3 shows the change of the mean diameter and the integrated intensity in the

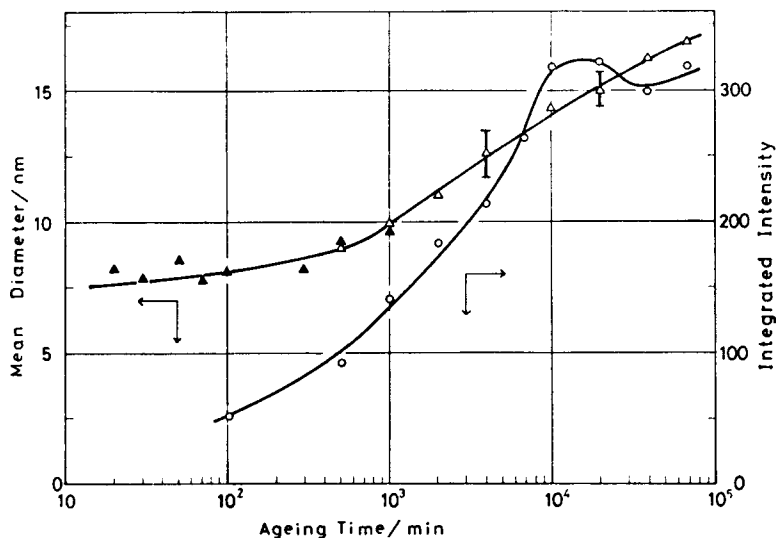


Fig. 3 Changes of the mean diameter and the integrated intensity during ageing at 408K, where the data ▲ are extracted from Ref. (25).

aged alloy at 408K. Within the time, in which only the GP zones exist, the mean size changed gradually. When the precipitation of the  $\theta''$  phase occurred beyond 500 min, both the mean diameter and the integrated intensity increased remarkably. Photo. 1 shows the TEM photograph of the  $\theta''$  precipitates at 4000 min. The dimension of the TEM image with its coherency strain corresponds to the result of the X-ray measurement. The integrated intensity decreased over 40000 min, at which a precipitation of the  $\theta'$  phase was observed. According to the result of the hardness measurement reported by Silcock<sup>15)</sup>, the peak hardness was obtained at about 30000 min for the Al-4.0wt%Cu alloy aged at 408K, and was associated with  $\theta''$  the phase with some  $\theta'$  precipitates. Boyd and Nicholson<sup>27)</sup> reported that the growth of  $\theta''$  precipitates obeys the particle coarsening process. In the present study, however, the integrated intensity as well as the mean size increased monotonically during the precipitation of the  $\theta''$  phase. This suggested that growth does not act on such a simple coarsening process.

(2) Reversion of  $\theta''$  Phase

The aged alloy at 408 for 4000 min was reverted in the temperature range from 448K to 523K. The change of diffuse scattering intensity during reversion at 488K is shown in Fig. 4. The intensity decreased with the reversion time until 10 min,

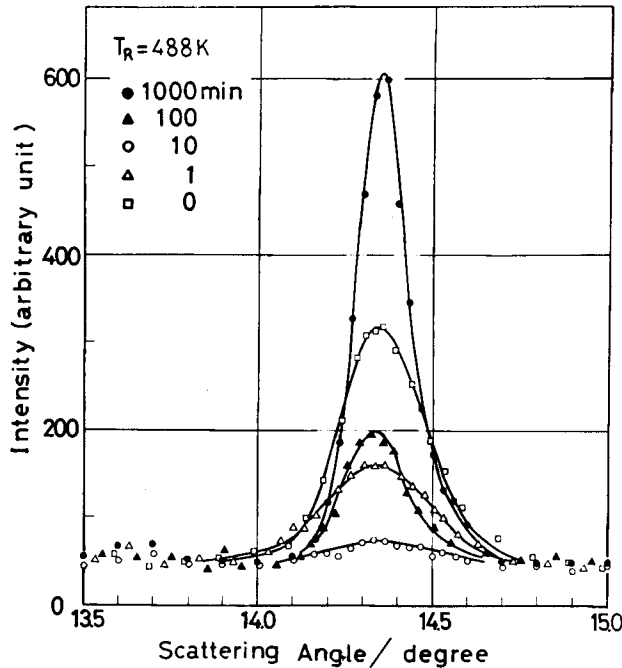


Fig. 4 Change of diffuse scattering intensity during reversion at 488K after ageing for 4000 min at 408K.

and then increased again. The half width of intensity profile after the 10 min reversion became narrower. According to the identification of the precipitated phase from the Laue photo, until the 10 min reversion, there existed only the  $\theta''$  phase. After that, the  $\theta'$  phase precipitated and its relative amount against the  $\theta''$  phase increased. Photo. 2 shows the structure of the reverted alloy at 488K for 20 min, where the major precipitates were of the  $\theta''$  phase, except a few of the  $\theta'$  phase. By comparison with Photo. 1, the size of the  $\theta''$  precipitates was slightly smaller and its number largely decreased. As shown in Photo. 3, the structure of the reverted alloy at 488K for 1000 min, the main precipitates were already of the  $\theta'$  phase, around which the misfit dislocation<sup>28)</sup> was observed.

Fig. 5 shows the change on the integrated intensity during reversion at various temperatures after ageing for 4000 min at 408K. All the reversion curves are similar to each other, where the initial decrease is due to the dissolution of the  $\theta''$  precipi-



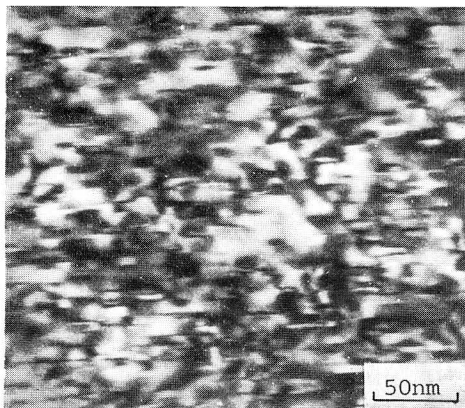


Photo. 1 Electron micrograph of the alloy, water quenched from 823K and aged for 4000 min at 408K, showing  $\theta''$  precipitates.

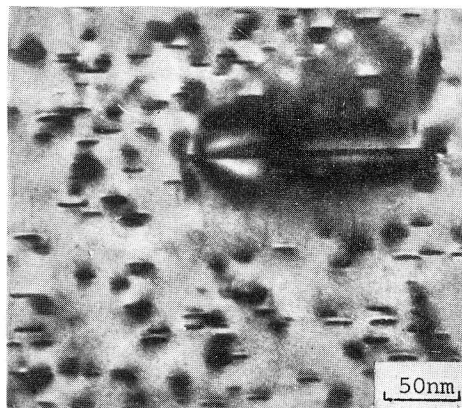


Photo. 2 Electron micrograph of the alloy reverted for 20 min at 488K after ageing for 4000 min at 408K, showing the homogeneously distributed  $\theta''$  precipitates and the large  $\theta'$  precipitates.

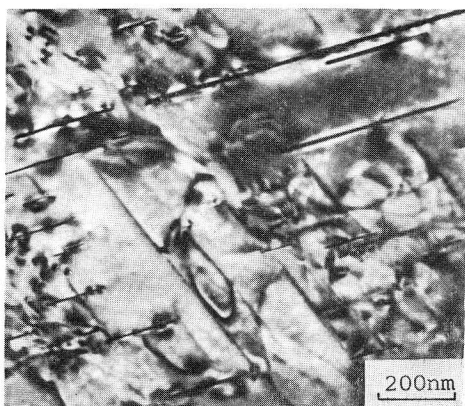


Photo. 3 Electron micrograph of the alloy reverted for 1000 min at 488K after ageing for 4000 min at 408K, showing the  $\theta'$  precipitates and a small amount of  $\theta''$  precipitates.

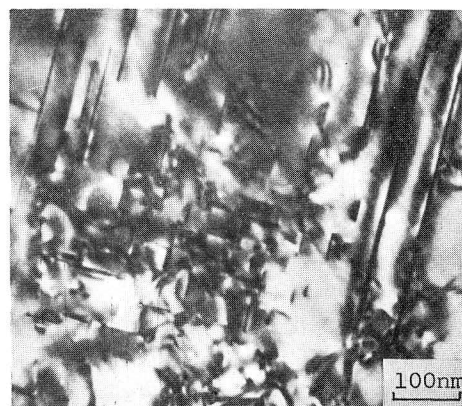


Photo. 4 Electron micrograph of the alloy reverted for 1000 min at 463K after ageing for 4000 min at 408K, showing the coexistence of  $\theta''$  and  $\theta'$  precipitates.

tates and the later increase due to the precipitation of the  $\theta'$  phase. Photo. 4 shows the structure of the reverted alloy at 463K for 1000 min, where both the  $\theta''$  and  $\theta'$  precipitates coexisted. When the alloy was reverted at a higher temperature, the time reaching to the minimum integrated intensity was accelerated and a larger decrease was observed. It should be, however, pointed out that the integrated intensity was not reduced to zero at any reversion temperature. The activation energy with respect

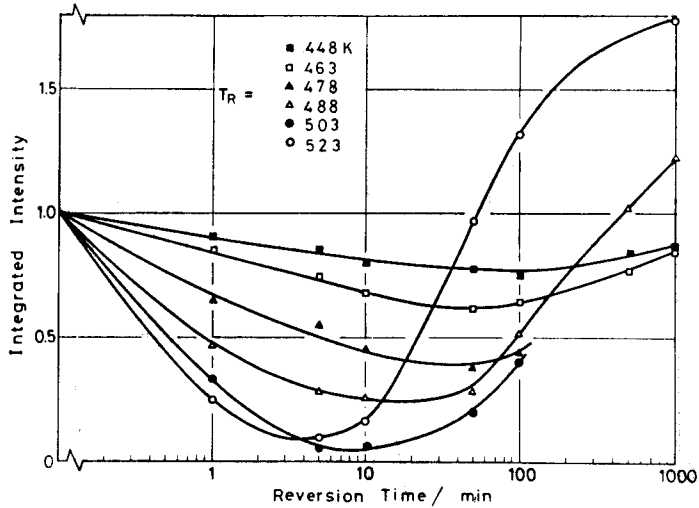


Fig. 5 Time dependence of integrated intensity during reversion after ageing for 4000 min at 408K.

to the dissolution of the  $\theta''$  precipitates was obtained to be 1.00eV by applying the Johnson-Mehl relation to the decreasing rate of the integrated intensity within the initial one minute reversion.

The change on the mean diameter of precipitates during reversion is shown in Fig. 6. The mean size decreased slightly at the initial stage although the integrated intensity decreased remarkably. Its decreasing rate was larger at the higher rever-

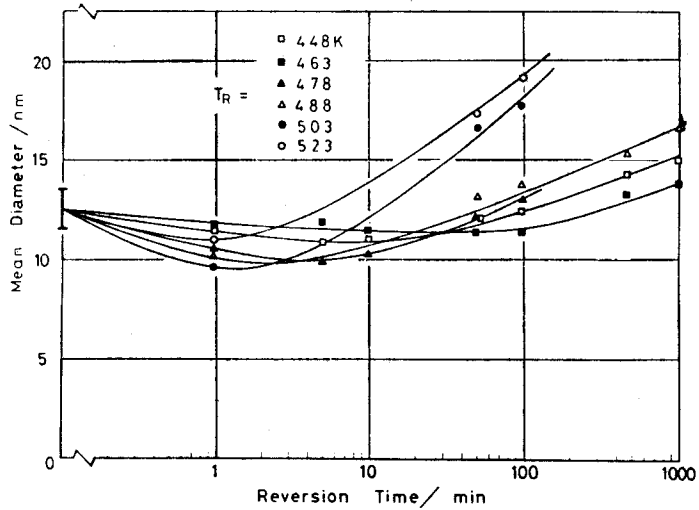


Fig. 6 Change of mean diameter during reversion after ageing for 4000 min at 408K.

sion temperature, except in the case of the 523K reversion. After the 10 min reversion, the mean size increased, depending on the precipitating rate of the  $\theta'$  phase. In particular at 503 and 523K, its increasing rate was very high.

### (3) Reversion of GP Zones

The precipitated phase in the aged alloy at 373K for 1000 min was only the GP zones, and their mean diameter was about 8.0 nm. Fig. 7 shows the change on

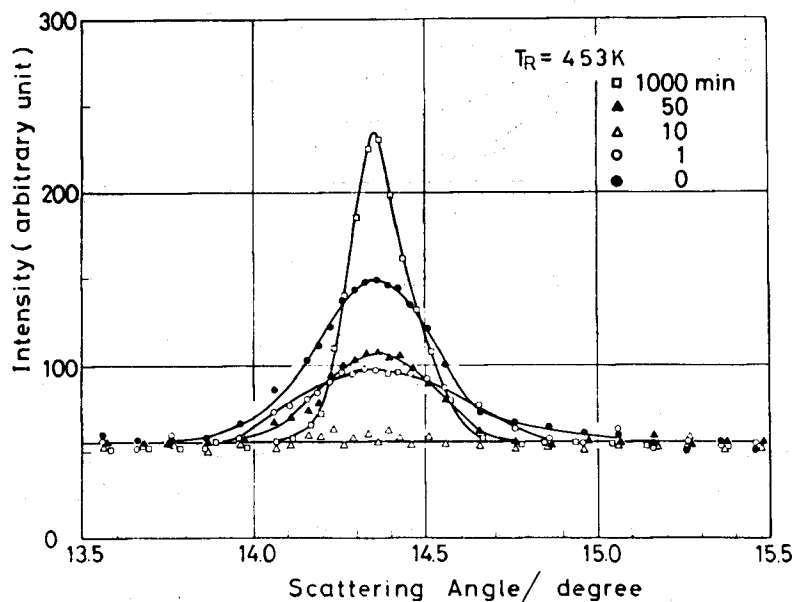


Fig. 7 Change of diffuse scattering intensity during reversion at 453K after ageing for 1000 min at 373K.

the diffuse scattering intensity during reversion at 453K. The diffuse scattering intensity decreased remarkably at 1 min and almost disappeared at 10 min. Hereafter the intensity recovered beyond 50 min. The half width of intensity profile became narrower after the 10 min reversion. The intensity profile was found to be asymmetric at 1000 min.

Fig. 8 shows the change on the integrated intensity during reversion. At 463K, the diffuse scattering was not yet observed at the one minute reversion, at which the GP zones dissolved completely. Below 453K, the integrated intensity decreased toward the minimum and again increased. This change arose from the super-imposition of both the dissolution of the GP zones and the precipitation of the  $\theta''$  phase. The activation energy for the dissolution of the GP zones was determined to be 0.94eV.

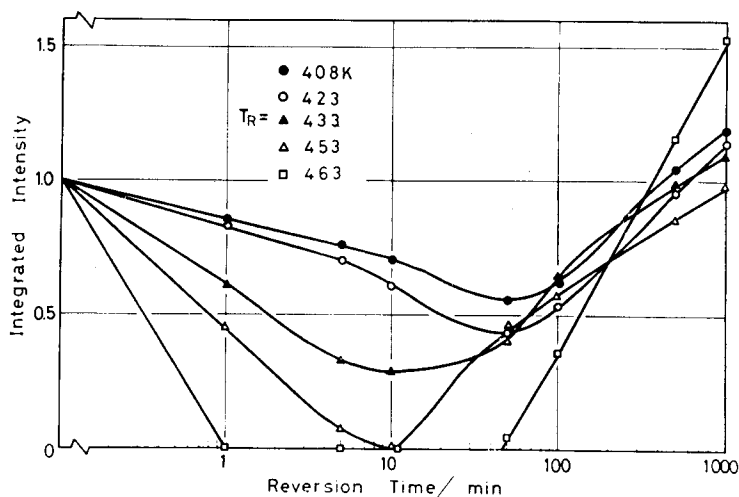


Fig. 8 Time dependence of integrated intensity during reversion after ageing for 1000 min at 373K.

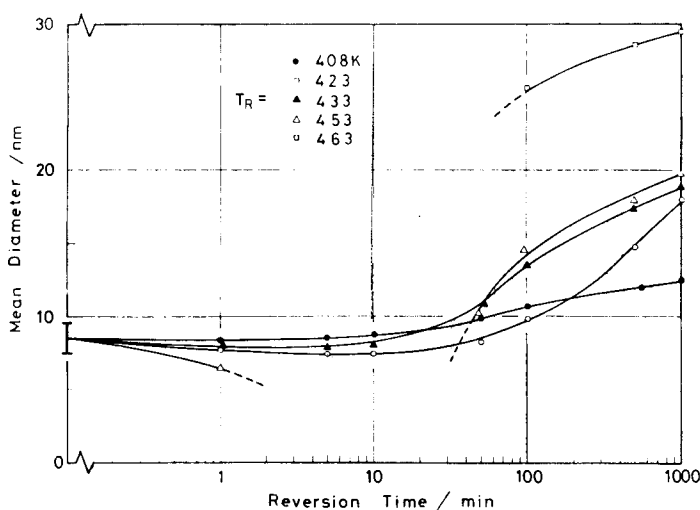


Fig. 9 Change of mean diameter during reversion after ageing for 1000 min at 373K.

The change on the mean diameter of the precipitates during reversion is shown in Fig. 9. When the alloy was reverted below 433K, the mean size remained nearly constant up to 10 min, and then increased gradually. At 463K, the mean diameter changed abruptly to 25.0 nm after the complete reversion.

Here we consider the successively precipitated phase after the dissolution of the GP zones. As shown in Fig. 8, the time, at which the integrated intensity

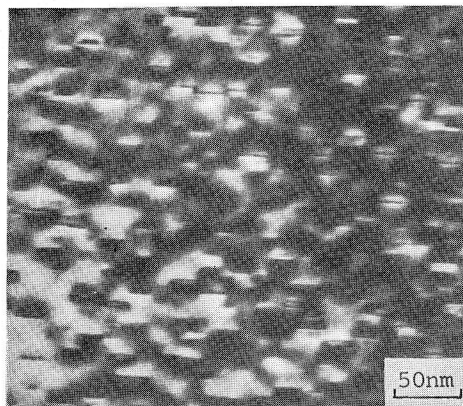


Photo. 5 Electron micrograph of the alloy reverted for 1000 min at 433K after ageing for 1000 min at 373K, showing only the precipitation of  $\theta''$  phase.

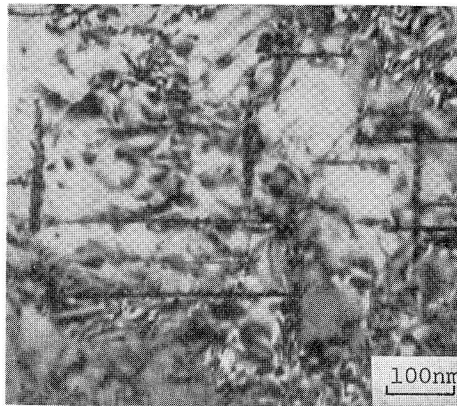


Photo. 6 Electron micrograph of the alloy reverted for 1000 min at 463K after ageing for 1000 min at 373K, showing only the precipitation of  $\theta'$  phase.

reached the minimum, was accelerated by the reversion at higher temperatures up to 433K. The recovery of the intensity began at an earlier time. Photo. 5 shows the structure of the reverted alloy at 433K for 1000 min. The precipitates were confirmed to be of the  $\theta''$  phase. Accordingly, the recovery of the integrated intensity was found to occur when accompanying the precipitation of the  $\theta''$  phase. On the other hand, at 463K, at which the GP zones were completely dissolved, the recovery of the intensity retarded in comparison with the cases below 433K. The time dependency of the change of the mean diameter at 463K was very different from the other cases. Photo. 6 shows the structure of the reverted alloy at 463K for 1000 min, where the precipitates were only of the  $\theta'$  phase. It should be noted that the two structures shown in Photos 4 and 6 are quite different in spite of the same reversion conditions. From the above experimental results, it was suggested that the precipitation of the  $\theta'$  phase occurs directly after the complete dissolution of the GP zones.

### III-2. Electrical Resistivity

#### (1) Reversion of GP Zones

The electrical resistivity of the as-quenched specimen was  $(1.575 \pm 0.005) \times 10^{-8} \Omega\text{m}$  at 77K after 5sec holding in ice-water. The residual resistivity in the Al-Cu binary alloy has been experimentally reported by some authors<sup>29),30),31)</sup> and may be adopted as being  $0.78 \times 10^{-8} \Omega\text{m/at}\% \text{Cu}$ . The theoretical value is reported as  $0.86 \times 10^{-8} \Omega\text{m/at}\% \text{Cu}$ <sup>32)</sup>. At 77K, the electrical resistivity for pure aluminium is  $0.237 \times 10^{-8} \Omega\text{m}$ <sup>33)</sup>. Therefore, the total resistivity for the Al-4wt%Cu solid solution alloy is  $1.56 \times$

$10^{-8}\Omega\text{m}$  at 77K, where the contribution from the solute atom was calculated by using Nordheim's law. Such an extrapolation of the resistivity to high copper concentration is reasonable up to about 3.7at%Cu, at which the Fermi surface does not exist in the third Brillouin zone because of the contraction of the Fermi sphere with an increase of copper concentration. The observed electrical resistivity for the as quenched specimen was slightly larger than the theoretical value. This difference seemed to arise from the quenched-in vacancy and/or the fine zones precipitated during quenching. The maximum contribution from the excess vacancies to the electrical resistivity is about  $0.01 \times 10^{-8}\Omega\text{m}$ , assuming that all the vacancies were frozen in.

Fig. 10 shows the resistivity change during reversion after ageing at 373K for

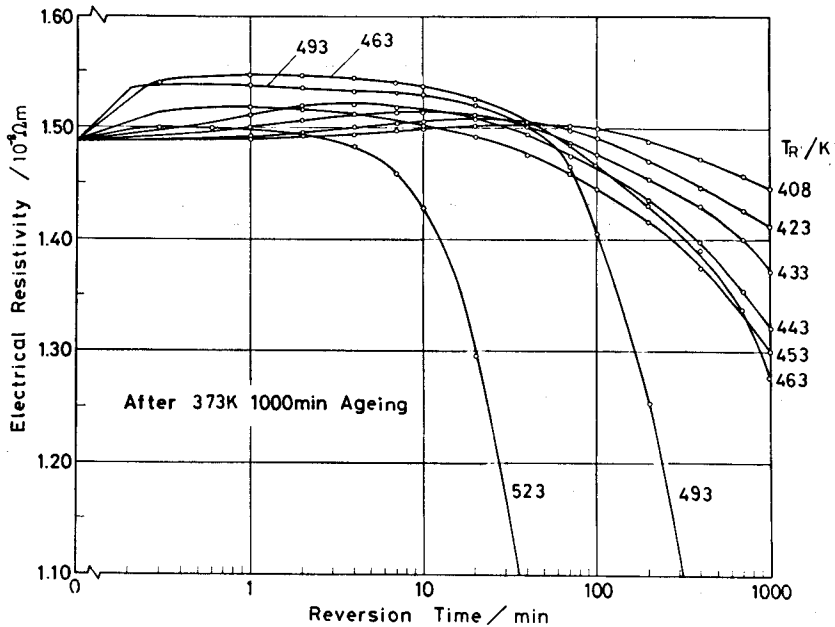


Fig. 10 Resistivity change during reversion after ageing for 1000 min at 373K.

1000 min, where the resistivity for the pre-aged specimen was  $(1.48 \pm 0.01) \times 10^{-8}\Omega\text{m}$ . The resistivity first increased at all the reversion temperatures, and reached each maximum. The maximum value became larger at higher reversion temperatures up to 463K, beyond which the maximum value decreased again. The highest value appeared at 463K and was  $1.55 \times 10^{-8}\Omega\text{m}$ . In its reversion, the GP zones dissolved completely and none of the precipitates appeared, as shown in Fig. 8. Above its critical temperature, for example, at 523K, the maximum value became again small. Fig. 11 shows the isoresistivity curve as a function of the reciprocal reversion temperature from the result of Fig. 10. Those curves could be divided into two regions.

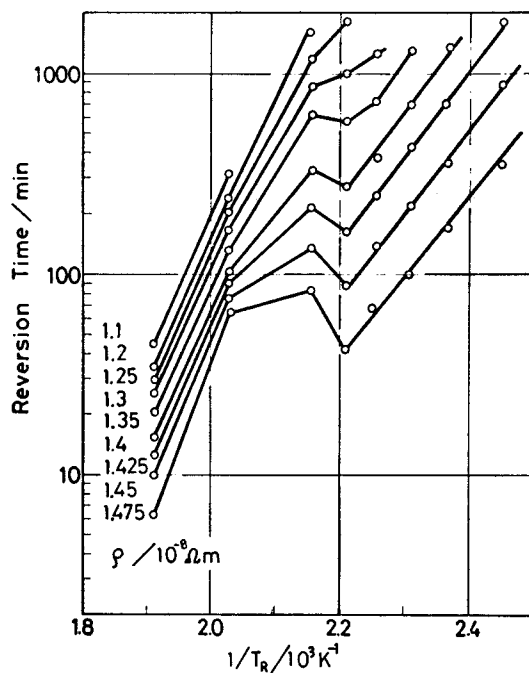


Fig. 11 Iso-resistivity curve as a function of reciprocal reversion temperature.

From the higher temperature region, the activation energy was obtained as 1.30eV. From the X-ray measurement and TEM observation, this region was governed by the precipitation of the  $\theta'$  phase. From the low temperature region, which corresponds to the precipitation of the  $\theta''$  phase, the activation energy was obtained as 0.95eV.

## (2) Reversion of $\theta''$ Phase

The electrical resistivity was  $(1.31 \pm 0.01) \times 10^{-8} \Omega m$  for the aged alloy at 408K for 4000 min. Fig. 12 shows the resistivity change during reversion. In all cases, the resistivity increased and reached the maximum. Its initial increase means the dissolution of the  $\theta''$  phase, and the final decrease corresponds to the precipitation of the  $\theta'$  phase. The time reaching to the maximum was accelerated and its absolute value became larger with an increase of the reversion temperature. The highest value, however, was  $1.46 \times 10^{-8} \Omega m$  at 548K and did not recover until the as-quenched value. The iso-resistivity curve obtained from the data of Fig. 12 is shown in Fig. 13. At the higher temperature region, the slope was the same for the three curves in spite of the different values of resistivity. The activation energy was 1.27eV. The precipitation of the  $\theta'$  phase was confirmed to occur in this region.

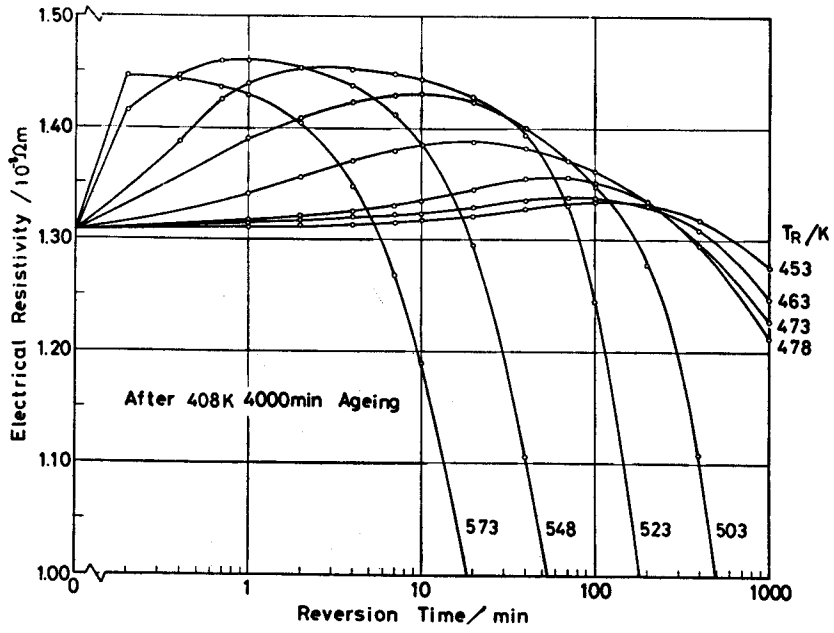


Fig. 12 Resistivity change during reversion after ageing for 4000 min at 408K.

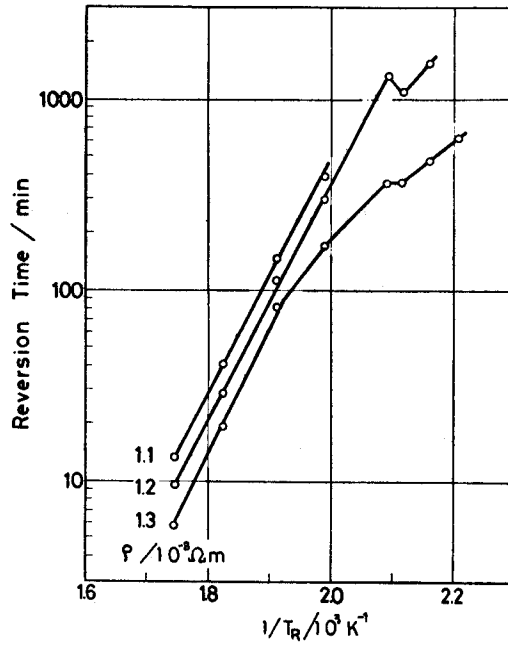


Fig. 13 Iso-resistivity curve as a function of reciprocal reversion temperature after ageing for 4000 min at 408K.



## IV. Discussion

In the reversion of the GP zones, both the minimum of integrated intensity and the maximum of resistivity appeared at the same reversion time as shown in Fig. 14.

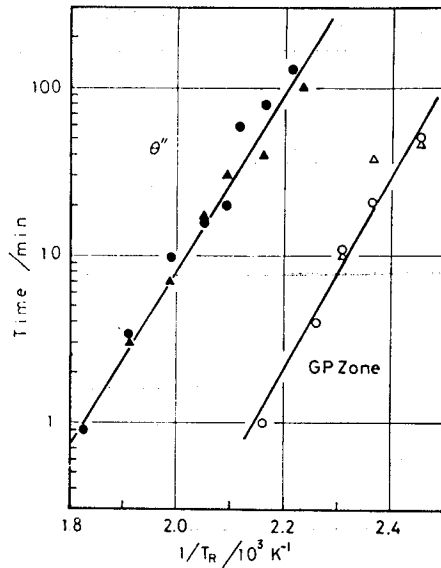


Fig. 14 The time reaching to the extreme value as a function of the reciprocal reversion temperature where  $\circ$  and  $\bullet$  are related to the resistivity maximum, and  $\triangle$  and  $\blacktriangle$  correspond to the minimum integrated intensity.

Also the same situation occurred for the reversion of the  $\theta''$  phase. The minimum of integrated intensity means that the total volume fraction of precipitation has reached the minimum. On the other hand, the change of the electrical resistivity arises from the solute atom in the matrix and the precipitates. When the mean size of precipitates is larger than several nanometers, the resistivity from the precipitates is proportional to the volume fraction and is smaller than the contribution from the solute atoms in the matrix<sup>34</sup>. Even if the precipitates become small by dissolving partially, the contribution to the resistivity is also small because the number of precipitates is very few. Therefore, the change of resistivity during reversion depends approximately on the concentration of the solute atom in the matrix. The maximum resistivity corresponds to the maximum concentration of the solute atom in the matrix. It is very reasonable that two observables, the integrated intensity and the resistivity, reach the extreme values at the same time.

Fig. 15 shows the minimum integrated intensity and the maximum resistivity as

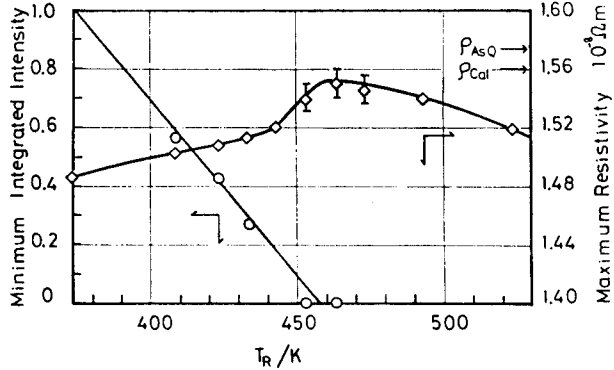


Fig. 15 Minimum integrated intensity and maximum electrical resistivity as a function of reversion temperature in each reversion after ageing for 1000 min at 373K.

functions of the reversion temperature for the dissolution of the GP zones. The minimum value of the integrated intensity decreased with temperature and reached zero at 458K. The maximum resistivity has a highest value around its temperature. It was  $1.55 \times 10^{-8} \Omega m$  and coincides almost with the theoretical value for the solid solution, but is slightly smaller than the as-quenched value. Therefore, the temperature for the complete dissolution of the GP zones was concluded to be 458K.

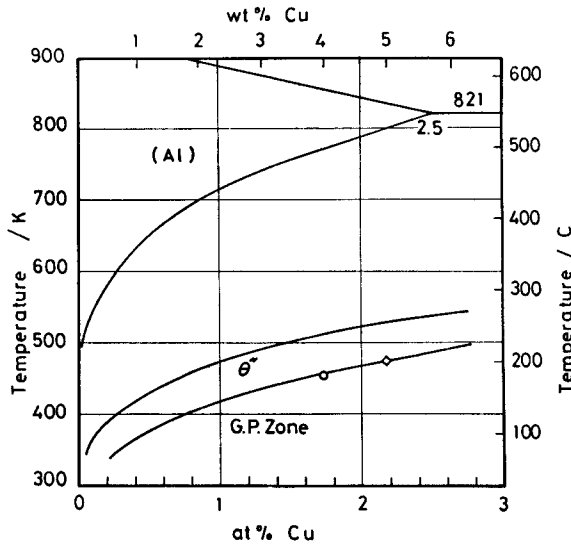


Fig. 16 Metastable phase diagram in the Al-Cu binary system, where two solid curves for GP zone and  $\theta''$  phase are referred to Beton and Rollason<sup>3)</sup>, and the signs  $\diamond$  and  $\circ$  are the experimental result reported by Gerold<sup>5)</sup> and the present data, respectively.

As shown in Fig. 16, this temperature was the same as that reported by Beton and Rollason<sup>8)</sup>, where the aged Al-4wt%Cu alloy at room temperature for 10 days, at which the mean diameter was about 5.0 nm, was reverted. In the present work, the mean diameter for the aged alloy at 373K for 1000 min was 8.0 nm. The reversion temperatures are the same for the GP zones with those diameters. In other words, the reversion temperature for the GP zones grown under 373K or less is constant. Gerold<sup>5)</sup> reported that the reversion temperature for the Al-5wt%Cu alloy is 473K. This report supports our consideration, but is in opposition with the result of Asano and Hirano<sup>11)</sup>.

Fig. 17 shows the temperature dependence of the extreme values of both the

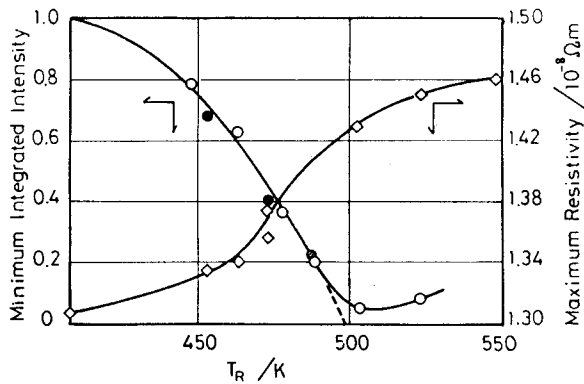


Fig. 17 Minimum integrated intensity and maximum electrical resistivity as a function of reversion temperature in each reversion after ageing at 408K, where  $\Delta$  and  $\circ$  show 4000 min ageing and  $\bullet$  shows 20000 min ageing, respectively.

integrated intensity and the electrical resistivity, including the results of two preceding ageing times at 408K for 4000 and 20000 min. When the curve of the integrated intensity is extrapolated to the horizontal axis, the intersection is 498K. However, the experimental integrated intensity did not reach zero. As shown in Photo. 2, the precipitation of the  $\theta''$  phase occurred already before the absolute minimum of the integrated intensity. All the maximum electrical resistivities for the reverted alloys are lower than the as-quenched value. This means that the concentration of copper atom in the matrix is low in comparison with the alloy concentration. The temperature, at which the total volume fraction of precipitates or the minimum integrated intensity becomes lowest, is defined as "a virtual reversion temperature." Its value for the  $\theta''$  phase is around 498K at which the resistivity was  $1.43 \times 10^{-8} \Omega m$ , and then the matrix concentration of the solute atom was estimated to be 3.6wt%Cu. Beton

and Rollason<sup>8)</sup> obtained the same result for the reverted alloy after ageing at 408K for 10 days, where almost all of the precipitates are of the  $\theta''$  phase. In the present case, the virtual reversion temperature is decided by the competitive reactions of both the dissolution of the  $\theta''$  phase and the precipitation of the  $\theta'$  phase.

Shimizu and Kimura<sup>18)</sup> discussed the activation energy during reversion in the Al-Cu alloy on the basis of the vacancy cluster mechanism<sup>21)</sup>. The diffusion of the copper atom is controlled by the vacancy concentration in the matrix. At the initial stage of reversion, the vacancy concentration is equal to that just after the preceding ageing treatment (region I). After that the vacancy concentration increases up to the critical value equilibrated with the dislocation loops having a small radius (or voids) (region II). When the reversion progressed and the dislocation loops grew, the vacancy concentration decreased to the thermally equilibrated value, regardless of the existence of dislocation loops (region III). The activation energy at each region was suggested<sup>18)</sup> to be 0.5, 1.0 and 1.3 eV, respectively. If the formation energy of the vacancy is 0.702 eV<sup>35)</sup>, each value varies to 0.5, 0.9 and 1.2 eV, respectively. The activation energy of the dissolution of the GP zones obtained from the decreasing rate of the integrated intensity as mentioned in Fig. 8 was 0.94 eV, and corresponds to region II. This means that the reaction of dissolution is controlled by an excess vacancy. The activation energy for the dissolution of the  $\theta''$  phase was 1.00 eV and its period corresponds to region II. The precipitation of the  $\theta'$  phase, for which the activation energy was 1.3 eV, occurs while being controlled by the concentration of thermal vacancy. As shown in Fig. 11, the activation energy for the precipitation of the  $\theta''$  phase after the dissolution of the GP zones was 0.95 eV. This value suggests an excess vacancy during the reaction, because excess vacancies are released accompanying the dissolution of the GP zones<sup>22), 23)</sup>.

In the Al-Cu binary alloy, three kinds of intermediate phases appear as GP zones,  $\theta''$  and  $\theta'$  phases. The phenomenological knowledge on the sequence of precipitation was made clear as follows. In general, during ageing or reversion, the successive precipitation occurs as GP zones  $\rightarrow \theta'' \rightarrow \theta'$ . For example, during reversion below 453K after ageing at 373K for 1000 min, the precipitation of the  $\theta''$  phase occurs after the partial dissolution of the GP zones. On the other hand, after the complete reversion of the GP zones, the  $\theta''$  phase does not precipitate, but the  $\theta'$  phase appears directly. This was made clear from Photos 4 and 6<sup>36)</sup>. Two possible mechanisms on the nucleation of the  $\theta'$  phase have been reported. Heimendal and Wassermann<sup>37)</sup> mentioned that sufficiently large  $\theta''$  precipitates act as the nucleation site of the  $\theta'$  phase. In another case, dislocations<sup>38), 39), 40)</sup>, subgrain boundary<sup>41)</sup> and dislocation loops<sup>42)</sup> act as the heterogeneous nucleation site. The fact that the  $\theta'$  phase precipitates without  $\theta''$  precipitates corresponds to the latter heterogeneous

nucleation. Therefore the  $\theta'$  phase occurs according to the following mechanism. As the activation energy was 1.3eV during the growth of the  $\theta'$  phase, sufficiently grown dislocation loops or voids serve as the nucleation site and the diffusion of the copper atom is carried out by the aid of thermal vacancies.

## V. Conclusion

When the Al-4.0wt%Cu alloy was aged at 373K for 1000 min, GP zones precipitated and their mean diameter was 8.0 nm. Hereafter during reversion, the reversion temperature, at which the GP zones dissolve completely, was found to be 458K. Its value coincides with the result reported by Beton and Rollason. After the complete reversion of the GP zones, above 463K, the  $\theta'$  phase precipitated directly, where precipitates are suggested to nucleate heterogeneously on the dislocation loops or voids. During reversion below 453K, both the minimum of integrated intensity and the maximum of electrical resistivity appeared simultaneously. It was understood to be the result of the superimposition of both the dissolution of the GP zones and the precipitation of the  $\theta''$  phase.

On ageing at 408K for 4000 min, the  $\theta''$  phase precipitated and the mean diameter was 12.5 nm. During the successive reversion at various temperatures, the integrated intensity did not reach zero. The extreme values of the integrated intensity and the resistivity occurred at the same time. This result was brought about by the superimposition of both the dissolution of the  $\theta''$  phase and the precipitation of the  $\theta'$  phase. The virtual reversion temperature, at which the total volume fraction of precipitates becomes minimum, was 498K.

## References

- 1) A. Guinier : Nature, **142** (1938), 569.
- 2) G. D. Preston : Phil. Mag., **26** (1938), 855.
- 3) A. Kelly and R. B. Nicholson : Progress in Materials Science, ed. by B. Chalmers, vol. 10, Pergamon Press, (1963), 151.
- 4) M. V. L. Gayler : J. Inst. Metals, **28** (1922) 213.
- 5) V. Gerold : Z. Metallk., **45** (1954), 593.
- 6) J. L. Meijering : Rev. Met., **49** (1952), 906.
- 7) R. Baur : Z. Metallk., **57** (1966), 275.
- 8) R. Beton and E. C. Rollason : J. Inst. Metals, **86** (1957-1958), 17.
- 9) V. Prakash and R. B. Nijihawan : J. Inst. Metals, **94** (1966), 180.
- 10) H. Iwasaki and K. Hirano : Trans. JIM, **5** (1964), 162.
- 11) K. Asano and K. Hirano : Japan J. Inst. Metals, **35** (1971), 364.
- 12) H. Hori and K. Hirano : Japan J. Inst. Metals, **37** (1973), 142.
- 13) R. Graf : J. Inst. Metals, **86** (1957-58), 534.
- 14) H. K. Hardy and T. J. Heal : Progress in Metal Physics, vol. 5, Pergamon Press, (1954), 143.
- 15) J. M. Silcock, H. K. Hardy and T. J. Heal : J. Inst. Metals, **82** (1953-54), 239.

- 16) R. B. Nicholson and J. Nutting : *Phil. Mag.*, **3** (1958), 531.
- 17) R. B. Nicholson, G. Thomas and J. Nutting : *J. Inst. Metals*, **87** (1958-59), 429.
- 18) H. Shimizu and H. Kimura : *Mater. Sci. Eng.*, **5** (1969-70), 127.
- 19) M. S. Anand, S. P. Murarka and R. P. Agarwala : *J. Appl. Phys.*, **36** (1965), 3860.
- 20) D. Turnbull, H. S. Rosenbaum and H. N. Treafis : *Acta Met.*, **8** (1960), 277.
- 21) J. Okamoto and H. Kimura : *Mater. Sci. Eng.*, **4** (1969), 39.
- 22) E. W. Hart : *Acta Met.*, **6** (1958), 533.
- 23) T. Federighi and G. Thomas : *Phil. Mag.*, **7** (1962), 127.
- 24) R. Baur and V. Gerold : *Z. Metallk.*, **57** (1966), 181.
- 25) T. Hirouchi, K. Ryu and Y. Murakami : *Japan J. Inst. Metals*, **37** (1973), 1120.
- 26) V. Gerold : *Z. Metallk.*, **45** (1954), 599.
- 27) J. D. Boyd and R. B. Nicholson : *Acta Met.*, **19** (1971), 1379.
- 28) G. C. Weatherly and R. B. Nicholson : *Phil. Mag.*, **17** (1968), 801.
- 29) F. Pawlek and K. Reichel : *Metall*, **12** (1958), 1.
- 30) D. Altenpohl : *Aluminium und Aluminium Legierungen*, Springer Verlag, (1965), 446.
- 31) W. A. Harrison : *Pseudo-Potentials in the Theory of Metals*, W. A. Benjamin, New York, (1966), 150.
- 32) Y. Fukai : *Phy. Rev.*, **186** (1969), 697.
- 33) K. Osamura, Y. Hiraoka and Y. Murakami : *Phil. Mag.*, **28** (1973) 321.
- 34) Y. Hiraoka, K. Osamura and Y. Murakami : *Japan J. Inst. Metals*, **40** (1976), 1233.
- 35) K. Furukawa, J. Takamura, N. Kuwana, R. Tahara and M. Abe : *J. Phys. Soc. of Japan*, **41** (1976), 1584.
- 36) A. Zahra-Kubik, M. Laffitte, P. Vigier und M. Wintenberger : *Aluminium*, **52** (1976), 357.
- 37) M. Heimendal and G. Wassermann : *Z. Metallk.*, **54** (1963), 385.
- 38) G. Thomas and J. Nutting : *Acta Met.*, **7** (1959), 515.
- 39) R. B. Nicholson : *Proc. Eur. Reg. Conf. on Electron Microscopy, De Nederlandse Verenging voor Electronen microscopie*, (1961), 375.
- 40) J. M. Silcock : *Acta Met.*, **8** (1960), 589.
- 41) R. B. Nicholson, G. Thomas and J. Nutting : *Brit. J. Appl. Phys.*, **9** (1958), 23.
- 42) G. Thomas and J. Nutting : *The Mechanism of Phase Transformations in Metals*, *Inst. Metals*, (1956), 172.
- 43) F. Nakamura, N. Matsumoto, K. Furukawa and J. Takamura : *Phil. Mag.*, **36** (1977), 1355.
- 44) W. F. Hosford and S. P. Agrawal : *Met. Trans.* **6A** (1975), 487.